Eur. J. Mineral.
2004, **16**, 335-344

Crystal chemistry of the schorl-dravite series

FERDINANDO BOSI and SERGIO LUCCHESI*

Dipartimento di Scienze della Terra, Università di Roma "La Sapienza", P.le A. Moro 5, I-00186 Roma, Italy

Abstract: Nineteen tourmaline samples of various provenances and geological settings were studied by EMPA, SREF and MS to represent the schorl-dravite compositional field. All samples belong to the Alkali group (except one with an *X*-site vacancy content of 0.53 apfu) and to the Oxy- and Hydroxy-subgroups. Among divalent cations, the main substitution involves ^{Y}Mg for ^{Y}Fe^{2+}, to produce the two end-members dravite and schorl.

Site populations were determined by a new minimization procedure that simultaneously accounts for both structural and chemical data. Results show that the crystals are characterized by disordered cation distribution between *Y* and *Z* sites: Al populates both sites, with a marked preference for the smaller *Z* octahedron; Mg is often equally distributed between *Y* and *Z*. Both Fe^{2+} and Fe^{3+} populate both *Y* and *Z* sites, but show a strong preference for *Y*. Specific mean bond distances (Å) optimised for major elements are: ^{Y}Al-O = 1.908, ^{Y}Mg-O = 2.084, ^{Y}Fe^{2+}-O = 2.139, ^{Z}Al-O = 1.900, ^{Z}Mg-O = 2.077 and ^{Z}Fe^{2+}-O = 2.131.

In the schorl-dravite solid solution, structural variations appear to be primarily due to *Y* and *Z* interactions. These effects are conspicuous over the entire structure, as *Y* dimensions directly affect the *a* cell parameter, while *Z* is similarly correlated with *c*. The dimensions of *Y* and *Z* octahedra are determined by Al contents. Dimensional variations of *Z* are well described by its bond-distance variations, except for *Z*-O7D. Both octahedra reciprocally interact, influencing their distortions: inverse correlations exist between *Y* dimension *vs. Z* quadratic elongation and *Z* dimension *vs. Y* quadratic elongation. As a common feature, the effects of the octahedral second coordination sphere are only confined to polyhedral distortions instead of dimensional variations, which only depend on site populations.

Key-words: Crystal structure, crystal-chemistry, disorder, schorl, dravite, tourmaline.

Introduction

The complexity of the crystal chemistry of tourmaline is easily appreciated by examining its structural formula with all of its possible site populations: $XY_3Z_6[T_6O_{18}](BO_3)_3V_3W$, where: *X* = Ca, Na, K, □; *Y* = Li, Mg, Fe^{2+}, Mn^{2+}, Al, Cr^{3+}, V^{3+}, Fe^{3+}, (Ti^{4+}); *Z* = Mg, Al, Fe^{2+}, Fe^{3+}, Cr^{3+}, V^{3+}; *T* = Si, Al, B; *B* = B, (□); *V* = OH, O; *W* = OH, F, O. The presence of vacancies, common in the *X* site, as well as light elements (Li, B, H) which cannot be determined by EMPA (Electron MicroProbe Analysis), and the consequent uncertainty in establishing the correct Fe^{2+}/Fe^{3+} ratio by stoichiometry, constitute the main difficulty in precise chemical characterization. Moreover, the occupancy of the same cation in different sites, as well as of cations with various oxidation states, does not allow unambiguous assessment of site populations. As a consequence, correct crystal-chemical characterization is achieved only by combining information from different techniques such as EMPA, MS (Mössbauer Spectroscopy) and SREF (Structure REFinement). Site assignment of various cations by means of bond distance and site scattering refinement information (Hawthorne *et al.*, 1993) allows complete understanding of tourmaline structure (Foit, 1989) in terms of geometrical relationships, intracrystalline cation distribution, and corresponding site preferences.

When assessing site populations to tourmaline, it is customary to assign Al to *Y* only after completely filling *Z* octahedron. While generally accepted for most tourmaline compositions, this procedure is not always considered to be valid in the case of schorl-dravite samples, because of inconsistencies between observed and calculated structural parameters, that demonstrate extensive cation (mostly Al and Mg) disorder (Grice & Ercit, 1993; Hawthorne *et al.*, 1993; Taylor *et al.*, 1995; McDonald & Hawthorne, 1995; Hawthorne, 1996; Bloodaxe *et al.*, 1999). Instead, Pieczka (1999, 2000) suggested that the influence of the second coordination sphere should also be considered, particularly between *Y* and *Z* octahedra, because they share a common edge (O3-O6) and may mutually influence polyhedral dimensions, thus "... excluding the possibility of *significant* disordering of octahedral divalent ions and Al in *Z* site ..." (Pieczka, 1999).

As octahedral cations like Al, Mg and Fe are expected to be particularly important in establishing intracrystalline disorder, this paper deals with the crystal chemistry of

*E-mail: sergio.lucchesi@uniroma1.it

0935-1221/04/0016-0335 $ 4.50
DOI: 10.1127/0935-1221/2004/0016-0335

Table 1. Provenance of tourmaline samples.

Sample	Provenance	Source
TM507c	Olkhon (Lake Baikal), Siberia	Anna Koneva
TM507e	Olkhon (Lake Baikal), Siberia	Anna Koneva
TM504c	Olkhon (Lake Baikal), Siberia	Anna Koneva
TM9840c	Lake Baikal, Siberia	Anna Koneva
TM9840f	Lake Baikal, Siberia	Anna Koneva
TM9914b	Lake Baikal, Siberia	Anna Koneva
TM235a	Beresov Mine, Siberia	MMR 15003/235
TM235b	Beresov Mine, Siberia	MMR 15003/253
TM65e	Arendal, Norway	MMR 8810/65
TM60e	Bovey Tracy, Devonshire, England	MMR 8805/60
TM233g	Zillerthal, Tyrol, Austria	MMR 14840/233
TM501e	Kwale, Mombasa, Kenya	Giorgio Graziani
TM84a	Cooma, New South Wales, Australia	MMR 8829/84
TM112a	Haddam, Connecticut, U.S.A.	MMR 8857/112
TM112c	Haddam, Connecticut, U.S.A.	MMR 8857/112
TMl2ap	Cruzeiro, Minas Gerais, Brazil	Julio César-Mendes
TMl2al	Cruzeiro, Minas Gerais, Brazil	Julio César-Mendes
TMl3l	Cruzeiro, Minas Gerais, Brazil	Julio César-Mendes
TMl4aa	Cruzeiro, Minas Gerais, Brazil	Julio César-Mendes

MMR: Museo di Mineralogia, University of Rome "La Sapienza".

schorl-dravite samples, and develops a new model for optimisation of site populations that accounts for geometrical parameters. To this aim, 19 tourmaline samples (Table 1) of various provenances and geological settings were selected to cover the range of the schorl-dravite series.

Methods

X-ray diffraction and structural analysis

The tourmaline samples were crushed, and suitable equidimensional fragments (~ 0.2 mm) were handpicked, cemented on a glass capillary and mounted on a Siemens P4 four-circle single-crystal automated diffractometer for X-ray diffraction study (Table 2). Cell parameters (Table 3) were measured using 52 reflections (13 independent and their Friedel pairs, on both sides of the direct beam). Scan speed was variable (Table 2), depending on reflection intensity estimated with a pre-scan. Background was measured with a stationary crystal and counter at the beginning and end of each scan, in both cases for half of the scan time. Preliminary full reciprocal space exploration was accomplished: no violations of *R*3*m* symmetry were found.

Data reduction was performed with the SHELXTL-PC program. Intensities were corrected for Lorentz and polarization effects. Absorption correction was accomplished with a semi-empirical method (Table 2). Only reflections with $I > 2(\sigma)$ were used (Table 3) from the original set of 1819-1790 data, in a full matrix least-squares refinement, with unitary weights, in the *R*3*m* space group. Absolute configuration was evaluated according to Barton (1969) and starting coordinates and atom labels were taken from Foit (1989). During structural refinement, variable parameters were: scale factor, isotropic secondary extinction coefficient, atomic coordinates, site scattering values (expressed as mean atomic numbers, m.a.n.) of *X*, *Y*, *Z*, and *T* sites, and displacement factors. Three cycles of isotropic refinement were followed by anisotropic cycles until a convergence to satisfactory *R* values (1.51–2.24 %; Table 3). Selected interatomic distances and m.a.n. are listed in Table 4. The complete set of atomic coordinates and displacement factors is available from the authors on request.

No chemical constraints were applied during refinement. Scattering curves for neutral B, 50 % ionised Si, Al

Table 2. Parameters for X-ray data collection.

Determination of unit cell parameters	
Radiation	Mo-$K\alpha_1$ (0.70930 Å)
Reflections used	13 (Friedel pairs on both +2θ and –2θ)
Range	85° – 95° 2θ
Temperature	296 K
Diffraction intensity collection	
Radiation	Mo-$K\alpha$ (0.71073 Å)
Monochromator	High-crystallinity graphite crystal
Range	3° – 70° 2θ
Reciprocal space range	$0 \le h, k \le 26$ $-12 \le l \le 12$
Scan method	ω
Scan range	2.4° 2θ
Scan speed	Variable 2.93° – 29.30° 2θ/min
Temperature	296 K
Data reduction	
Refinement	SHELXTL – PC
Corrections	Lorentz, Polarization
Absorption correction	Semi-empirical, 13 Ψ scans (10° – 95° 2θ)

Table 3. Data collection and structural refinement information.

Sample	*a* (Å)	*c* (Å)	# refl.	EXT.	R_{all}
TM507c	15.9610(8)	7.2214(4)	1702	35(3)	1.83
TM507e	15.9521(8)	7.2167(5)	1700	33(3)	1.74
TM235a	15.9433(7)	7.2095(4)	1700	32(3)	1.93
TM235b	15.9388(8)	7.2050(5)	1700	28(3)	1.87
TM112a	15.9633(7)	7.1942(4)	1698	188(7)	2.14
TM112c	15.9636(7)	7.1911(4)	1698	132(6)	2.16
TM233g	15.9355(8)	7.2002(4)	1698	74(4)	1.86
TM501e	15.9267(8)	7.1991(4)	1692	164(5)	1.89
TM84a	15.9391(7)	7.1515(4)	1682	38(3)	1.51
TM60e	15.9856(8)	7.1840(6)	1702	8(2)	2.11
TM65e	15.9541(8)	7.2035(5)	1700	13(3)	2.17
TM504c	15.9706(10)	7.2276(7)	1706	11(2)	2.29
TMl2ap	15.9659(6)	7.1693(3)	1690	304(6)	2.08
TMl2al	15.9736(6)	7.1644(3)	1690	77(3)	1.74
TMl3l	15.9669(6)	7.1745(3)	1692	212(5)	2.24
TMl4aa	15.9664(6)	7.1758(3)	1692	230(5)	2.23
TM9840c	15.9341(8)	7.1890(5)	1696	72(4)	1.62
TM9840f	15.9303(7)	7.1951(4)	1696	70(4)	2.11
TM9914b	15.9821(7)	7.2215(4)	1708	31(3)	1.74

Notes: # refl. = number of observed independent reflections; EXT. = Isotropic secondary extinction coefficient (x 10^5); R_{all} = disagreement factor (%).

Table 4. Schorl-dravite series: selected bond distances (Å), site volumes (Å^3), quadratic elongations and m.a.n.

Sample	TM507c	TM507e	TM235a	TM235b	TM112a	TM112c	TM233g	TM501e	TM84a	TM60e	TM65e	TM504c	TMl2ap	TMl2al	TMl3l	TMl4aa	TM9840c	TM9840f	TM9914b
***B* site**																			
B-O2	1.374(2)	1.376(2)	1.372(2)	1.371(2)	1.368(2)	1.373(2)	1.372(2)	1.373(2)	1.363(2)	1.367(3)	1.371(3)	1.379(3)	1.366(3)	1.365(2)	1.365(3)	1.369(3)	1.372(2)	1.374(2)	1.376(2)
B-O8A x 2	1.376(1)	1.375(1)	1.376(1)	1.376(1)	1.381(1)	1.380(1)	1.377(1)	1.375(1)	1.380(1)	1.380(1)	1.378(1)	1.372(1)	1.381(1)	1.382(1)	1.382(1)	1.379(1)	1.3765(9)	1.376(1)	1.376(1)
<*B*-O>	1.375	1.375	1.374	1.375	1.376	1.377	1.375	1.374	1.374	1.376	1.376	1.375	1.376	1.376	1.376	1.375	1.375	1.376	1.376
m.a.n. *B*	5	5	5	5	5	5	5	5	5	5	5	5	5	5	5	5	5	5	5
***T* site**																			
T-O4	1.6283(4)	1.6286(4)	1.6266(4)	1.6258(4)	1.6292(5)	1.6287(5)	1.6267(4)	1.6232(4)	1.6221(4)	1.6267(5)	1.6269(5)	1.6300(5)	1.6249(5)	1.6268(4)	1.6253(5)	1.6255(5)	1.6260(4)	1.6256(5)	1.6286(4)
T-O5	1.6440(9)	1.6449(9)	1.6413(9)	1.6407(9)	1.646(1)	1.645(1)	1.6415(9)	1.6395(9)	1.6357(8)	1.640(1)	1.641(1)	1.647(1)	1.638(1)	1.6393(9)	1.640(1)	1.639(1)	1.6420(8)	1.6435(8)	1.6432(9)
T-O7	1.6033(9)	1.6025(8)	1.6044(8)	1.6058(8)	1.6085(9)	1.6079(8)	1.6051(8)	1.6029(8)	1.6112(7)	1.610(1)	1.6047(9)	1.602(1)	1.611(1)	1.6128(8)	1.611(1)	1.610(1)	1.6048(7)	1.6038(7)	1.6047(8)
T-O6	1.6049(8)	1.6035(8)	1.6050(9)	1.6057(9)	1.607(1)	1.607(1)	1.6082(9)	1.6087(9)	1.6106(9)	1.608(1)	1.607(1)	1.603(1)	1.609(1)	1.6102(9)	1.608(1)	1.608(1)	1.6072(8)	1.6072(8)	1.6059(9)
<*T*-O>	1.620	1.620	1.619	1.620	1.623	1.622	1.620	1.619	1.620	1.621	1.620	1.621	1.621	1.622	1.621	1.621	1.620	1.620	1.621
V_T	2.173(2)	2.172(2)	2.172(2)	2.173(2)	2.183(2)	2.182(2)	2.176(2)	2.170(2)	2.178(2)	2.181(2)	2.175(2)	2.174(3)	2.181(2)	2.187(2)	2.181(2)	2.180(2)	2.175(2)	2.174(2)	2.176(2)
$<\lambda_T>$	1.0029	1.0032	1.0024	1.0023	1.0028	1.0027	1.0024	1.0020	1.0010	1.0018	1.0023	1.0034	1.0014	1.0014	1.0016	1.0015	1.0023	1.0025	1.0026
m.a.n. *T*	14.04(5)	13.95(5)	13.88(5)	14.02(5)	13.96(6)	13.91(4)	13.92(5)	13.99(6)	13.94(4)	13.92(6)	13.95(5)	13.96(5)	13.91(6)	13.90(5)	14.00(6)	14.01(6)	13.89(4)	13.83(5)	13.76(5)
***X* site**																			
X-O2B,F x 3	2.501(2)	2.494(1)	2.471(2)	2.476(2)	2.482(2)	2.482(2)	2.483(2)	2.501(2)	2.543(3)	2.511(2)	2.479(2)	2.491(2)	2.517(3)	2.519(2)	2.504(3)	2.510(3)	2.504(2)	2.508(2)	2.475(2)
X-O4B,F x 3	2.798(1)	2.795(1)	2.831(1)	2.829(1)	2.806(1)	2.807(1)	2.822(1)	2.823(1)	2.820(1)	2.812(2)	2.826(1)	2.788(1)	2.822(2)	2.818(1)	2.821(2)	2.820(2)	2.809(1)	2.803(1)	2.821(1)
X-O5B,F x 3	2.710(1)	2.703(1)	2.747(1)	2.745(1)	2.725(1)	2.725(1)	2.734(1)	2.729(1)	2.756(1)	2.746(2)	2.742(1)	2.702(1)	2.757(2)	2.758(1)	2.754(2)	2.756(2)	2.719(1)	2.714(1)	2.741(1)
<*X*-O>	2.670	2.664	2.683	2.683	2.671	2.671	2.680	2.684	2.706	2.690	2.683	2.661	2.699	2.698	2.693	2.695	2.677	2.675	2.679
V_X	31.49(1)	31.264(9)	32.02(1)	32.04(1)	31.60(1)	31.576(9)	32.00(1)	32.03(1)	32.919(9)	32.27((1)	32.00(1)	31.15(1)	32.63(1)	32.593(8)	32.43(1)	32.48(1)	31.792(9)	31.722(9)	31.87(1)
m.a.n. *X*	11.9(1)	12.4(1)	10.8(1)	10.7(1)	11.8(1)	11.8(1)	11.1(1)	9.9(1)	6.0(1)	10.1(1)	10.8(1)	13.6(1)	7.9(1)	8.1(1)	8.8(1)	8.7(1)	10.7(1)	11.0(1)	12.2(1)
***Y* site**																			
Y-O1	1.974(1)	1.969(1)	1.994(1)	1.991(1)	2.007(1)	2.007(1)	1.978(1)	1.941(1)	1.998(1)	2.029(4)	1.981(4)	1.977(1)	2.013(2)	2.025(1)	2.018(2)	2.015(2)	1.975(1)	1.966(1)	2.000(1)
Y-O2B x 2	2.018(1)	2.017(1)	2.001(1)	1.999(1)	2.017(1)	2.015(1)	1.999(1)	1.996(1)	1.975(1)	2.008(1)	2.007(1)	2.029(1)	1.992(1)	1.995(1)	1.998(1)	1.997(1)	1.9986(9)	2.000(1)	2.023(1)
Y-O3	2.121(1)	2.123(1)	2.116(1)	2.113(1)	2.148(1)	2.148(1)	2.118(1)	2.122(1)	2.128(1)	2.164(1)	2.135(1)	2.131(2)	2.155(1)	2.160(1)	2.152(2)	2.152(2)	2.123(1)	2.122(1)	2.160(1)
Y-O6C x 2	1.9983(9)	1.9972(8)	1.9986(9)	1.9944(9)	2.013(1)	2.013(1)	1.9902(9)	1.9850(8)	2.0124(8)	2.0326(9)	2.003(1)	2.006(1)	2.024(1)	2.0288(8)	2.025(1)	2.024(1)	1.9942(8)	1.9901(8)	2.0210(9)
<*Y*-O>	2.021	2.020	2.018	2.015	2.036	2.035	2.012	2.004	2.017	2.046	2.023	2.030	2.034	2.039	2.036	2.035	2.014	2.011	2.041
V_Y	10.675(5)	10.657(5)	10.595(5)	10.548(5)	10.874(6)	10.868(5)	10.505(5)	10.379(6)	10.517(5)	11.008(9)	10.665(8)	10.823(6)	10.794(6)	10.873(5)	10.839(7)	10.826(7)	10.536(4)	10.500(4)	10.967(5)
$<\lambda_Y>$	1.0214	1.0215	1.0233	1.0233	1.0234	1.0234	1.0233	1.0232	1.0270	1.0250	1.0234	1.0209	1.0264	1.0266	1.0259	1.0256	1.0230	1.0227	1.0232
m.a.n. *Y*	15.12(9)	14.34(8)	15.06(5)	15.03(5)	16.06(7)	15.95(5)	14.67(5)	14.32(7)	18.44(7)	19.81(10)	16.00(7)	15.02(9)	19.64(11)	19.98(9)	19.46(10)	19.38(11)	14.69(5)	14.70(6)	19.03(8)
***Z* site**																			
Z-O3	1.999(1)	1.9968(9)	1.990(1)	1.9909(9)	1.987(1)	1.987(1)	1.9927(9)	1.9976(9)	1.9840(9)	1.984(1)	1.994(1)	1.998(1)	1.983(1)	1.9828(9)	1.984(1)	1.985(1)	1.9922(9)	1.992(1)	1.9900(9)
Z-O6	1.9094(9)	1.9074(8)	1.8977(9)	1.8970(9)	1.884(1)	1.883(1)	1.8963(8)	1.9063(9)	1.8764(8)	1.877(1)	1.895(1)	1.910(1)	1.875(1)	1.8703(8)	1.876(1)	1.877(1)	1.8958(8)	1.9011(9)	1.8925(8)
Z-O8	1.9336(8)	1.933(1)	1.9310(8)	1.9291(8)	1.9279(9)	1.9287(9)	1.9267(8)	1.9262(8)	1.9206(7)	1.9287(9)	1.9286(9)	1.935(1)	1.9241(9)	1.9258(8)	1.9262(9)	1.926(1)	1.9253(7)	1.9273(9)	1.9340(8)
Z-O7E	1.9127(9)	1.9126(9)	1.9042(9)	1.9038(9)	1.898(1)	1.898(1)	1.9036(9)	1.9078(9)	1.8868(8)	1.893(1)	1.904(1)	1.917(1)	1.889(1)	1.8860(9)	1.890(1)	1.891(1)	1.9020(8)	1.905(1)	1.9053(9)
Z-O7D	1.9645(9)	1.9634(9)	1.9605(9)	1.9580(9)	1.961(1)	1.961(1)	1.9575(9)	1.9564(9)	1.9548(8)	1.966(1)	1.961(1)	1.967(1)	1.960(1)	1.9587(9)	1.960(1)	1.960(1)	1.9572(8)	1.957(1)	1.9691(9)
Z-O8E	1.9026(8)	1.902(1)	1.8983(8)	1.8986(8)	1.8955(9)	1.8938(9)	1.8989(8)	1.8980(8)	1.8877(7)	1.8935(9)	1.8976(9)	1.9050(9)	1.8908(9)	1.8878(8)	1.8900(8)	1.891(1)	1.8967(7)	1.8959(8)	1.9004(8)
<*Z*-O>	1.937	1.936	1.930	1.930	1.926	1.925	1.929	1.932	1.918	1.924	1.930	1.939	1.920	1.919	1.921	1.922	1.928	1.930	1.932
V_Z	9.495(3)	9.480(4)	9.396(3)	9.382(3)	9.335(4)	9.333(3)	9.376(3)	9.410(4)	9.219(3)	9.316(4)	9.392(4)	9.525(5)	9.259(4)	9.234(3)	9.266(4)	9.278(4)	9.361(3)	9.381(3)	9.432(3)
$<\lambda_Z>$	1.0140	1.0139	1.0141	1.0143	1.0135	1.0135	1.0144	1.0149	1.0144	1.0131	1.0140	1.0134	1.0137	1.0136	1.0136	1.0136	1.0144	1.0145	1.0131
m.a.n. *Z*	13.42(6)	13.05(6)	13.08(4)	13.11(4)	13.12(5)	13.06(4)	13.07(4)	13.11(5)	13.31(4)	13.46(5)	13.01(5)	13.48(7)	13.29(5)	13.37(4)	13.35(5)	13.38(5)	12.87(4)	12.92(5)	13.16(4)

and O, fully ionised V^{3+}, Mg, Fe^{2+} and Na were used because they furnished the best values of conventional agreement factors over all $\sin\theta/\lambda$ intervals. This combination also gave satisfactory agreement (within 1 %) between values of total m.a.n. obtained by structural refinement and chemical analysis.

Chemical analysis and ^{57}Fe Mössbauer spectra

After X-ray data collection, the same crystals were mounted on glass slides, polished and carbon-coated for electron microprobe analysis (WDS-EDS method) on a CAMECA CX827 electron microprobe, operating at 15 KV and 15 nA (sample current) and with a 5 µm beam. Raw data was reduced using the ZAF and PAP (Pouchou & Pichoir, 1984) corrections. Natural and synthetic standards were used: anorthite (Al), rutile (Ti), olivine (Si, Fe), rhodonite (Mn), diopside (Mg, Ca), sphalerite (Zn), orthoclase (Na, K), fluorite (F), synthetic metals (Cr, V). From 10 to 15 point analyses were performed for each specimen along two orthogonal traverses. The chemical composition data (Table 5) are the average of the spot analyses and their standard deviations account for crystal homogeneity. Each element determination was accepted after checking that the intensity of analysed standard before and after each determination was within 1.00 ± 0.01. Precision for major elements (Al, Mg, Si, Fe) was within ~ 1% of the actual amount present; that for minor elements was within ~ 5%.

Iron speciation was determined by fitting Mössbauer spectra collected at 25°C using a conventional spectrometer system operating in constant acceleration mode with a ^{57}Co source of 50 mCi in rhodium matrix. Absorbers were prepared by pressing finely ground samples with a powdered acrylic resin (transoptic powder) to self-supporting discs. For the various samples, from 10 to 60 mg of tourmaline powder was used, depending on both sample availability and total iron contents, so as to have absorbers with an Fe thickness of 1-2 mg/cm^2. Data collection time was usually 1-2 days, but in a few cases spectra had to be collected for one week for good statistics. Spectral data for the velocity range –4 to +4 mm/s were recorded on a multichannel analyser using 512 channels. After velocity calibration against a spectrum of high-purity α-iron foil (25 µm thick), the raw data were folded to 256 channels. The spectra were fitted assuming Lorentzian peak shape, using the Recoil 1.04 fitting program. Reduced χ^2 was used as a parameter to evaluate statistical best fit, and uncertainties were calculated using the covariance matrix. Errors were estimated at about ± 0.02 mm/s for centre shift (d), quadrupole splitting (D) and peak width

Table 5. Schorl-dravite series: chemical composition (wt. %) based on EMPA and MS.

Sample	TM507c	TM507e	TM235a	TM235b	TM112a	TM112c	TM233g	TM501e	TM84a	TM60e	TM65e	TM504c	TMl2ap	TMl2al	TMl3l	TMl4aa	TM9840c	TM9840f	TM9914b
SiO_2	36.69(5)	36.2(2)	36.8(2)	36.9(1)	35.8(1)	35.9(2)	36.3(3)	37.2(1)	35.7(4)	35.7(1)	36.8(7)	36.0(2)	35.9(1)	35.4(4)	35.6(5)	36.2(3)	36.4(2)	36.8(2)	35.48(8)
TiO_2	0.19(2)	0.28(9)	0.4(2)	0.4(1)	0.43(2)	0.49(1)	0.27(7)	0.18(3)	0.22(1)	0.8(1)	0.34(1)	0.21(2)	0.6(1)	0.30(8)	0.34(4)	0.40(3)	1.07(6)	1.18(3)	0.73(5)
B_2O_3	10.7(5)	10.6(5)	10.7(5)	10.7(5)	10.6(5)	10.6(5)	10.7(5)	10.8(5)	10.5(5)	10.3(5)	10.7(5)	10.6(5)	10.5(5)	10.5(5)	10.4(5)	10.5(5)	10.7(5)	10.8(5)	10.4(5)
Al_2O_3	28.0(6)	29.3(5)	32.9(5)	33.0(4)	31.8(1)	32.3(3)	34.1(2)	32.8(2)	36.5(2)	31(1)	31.7(2)	27.0(3)	34.1(3)	34.3(5)	32.9(4)	33.0(2)	33.59(3)	33.4(1)	29.1(3)
Cr_2O_3	2.4(2)	1.2(1)	0.01(2)	0.01(2)	0.136(1)	0.11(2)	0.005(9)	0.06(1)	0.01(1)	0.002(2)	0.004(4)	1.30(7)	-	-	-	-	0.03(1)	0.06(1)	0.03(1)
V_2O_3	6.1(4)	3.8(2)	0.02(2)	0.02(2)	0.06(2)	0.07(3)	0.03(1)	0.02(2)	0.01(1)	0.052(5)	0.04(1)	6.4(2)	-	-	-	-	0.19(2)	0.28(3)	0.33(1)
FeO_{tot}	0.008(7)	0.02(1)	4.4(1)	4.1(1)	6.2(2)	5.5(4)	3.4(1)	4.05(9)	9.4(3)	12.2(8)	5.8(2)	0.05(3)	12.25(5)	12.6(2)	11.7(2)	11.5(2)	2.5(1)	2.2(3)	10.0(3)
MnO	0.00	0.002(4)	0.03(2)	0.01(1)	0.02(2)	0.05(3)	0.01(1)	0.02(2)	0.36(5)	0.09(2)	0.04(2)	0.01(1)	0.00	0.36(6)	0.15(5)	0.15(7)	0.08(4)	0.07(4)	0.01(1)
MgO	10.6(2)	11.0(3)	8.5(2)	8.6(1)	8.26(2)	8.38(9)	8.8(2)	9.08(8)	2.48(2)	3.7(6)	8.70(5)	11.4(1)	2.74(4)	2.1(2)	3.6(2)	3.7(1)	8.96(8)	9.28(6)	7.1(1)
ZnO	0.00	0.00	0.05(8)	0.05(6)	0.09(5)	0.00	0.07(4)	0.04(4)	0.10(6)	0.09(8)	0.07(3)	0.10(7)	0.11(6)	0.31(4)	0.2(1)	0.2(1)	0.1(1)	0.05(5)	0.04(6)
CaO	1.41(3)	1.9(4)	0.44(5)	0.5(1)	1.46(1)	1.50(2)	0.6(1)	0.043(8)	0.058(8)	0.5(3)	0.63(2)	2.34(4)	0.00	0.00	0.00	0.00	0.87(5)	1.08(1)	0.91(2)
Na_2O	1.45(3)	1.51(4)	2.38(6)	2.30(4)	1.76(2)	1.76(4)	2.28(6)	2.37(3)	1.41(4)	2.09(5)	2.15(3)	1.50(2)	1.98(1)	2.11(9)	2.25(5)	2.22(7)	1.93(5)	1.90(4)	2.25(4)
K_2O	0.060(7)	0.05(2)	0.022(8)	0.02(1)	0.008(8)	0.012(5)	0.018(7)	0.052(6)	0.03(1)	0.040(7)	0.05(1)	0.07(1)	0.06(1)	0.060(8)	0.03(1)	0.043(8)	0.050(7)	0.065(8)	0.022(6)
F	0.16(9)	0.10(7)	0.01(2)	0.09(5)	0.24(7)	0.12(8)	0.01(1)	0.04(2)	0.07(6)	0.4(1)	0.04(4)	0.6(1)	0.34(4)	0.34(7)	0.4(1)	0.30(1)	0.14(3)	0.11(3)	0.08(7)
H_2O	3.3(2)	3.2(2)	3.5(2)	3.3(2)	3.2(2)	3.2(2)	3.3(2)	3.2(2)	3.1(2)	3.1(2)	3.3(2)	3.0(1)	3.2(2)	3.2(2)	2.7(2)	2.9(2)	3.2(2)	3.2(2)	3.1(2)
Total	100.88	99.10	99.99	99.99	99.98	99.98	99.86	99.91	99.91	99.88	100.40	100.32	101.68	101.48	100.17	100.94	99.78	100.36	99.62
$Fe_2O_3^*$	-	-	0.63	0.60	2.27	2.03	1.25	4.41	1.15	2.23	2.91	-	0.68	0.70	5.72	4.09	-	-	4.35
FeO^*	-	-	3.79	3.61	4.15	3.71	2.29	0.08	8.37	10.16	3.20	-	11.64	11.94	6.55	7.82	-	-	6.13
Number of cations calculated on basis of 31 (O, OH, F)																			
Si	5.96(6)	5.95(6)	5.98(6)	5.98(5)	5.88(5)	5.88(5)	5.88(6)	6.00(5)	5.89(6)	6.00(9)	5.97(5)	5.92(5)	5.91(5)	5.87(7)	5.93(7)	5.98(6)	5.90(5)	5.93(5)	5.94(5)
Ti^{4+}	0.024(2)	0.03(1)	0.05(2)	0.05(1)	0.054(2)	0.061(2)	0.033(9)	0.022(3)	0.027(1)	0.11(1)	0.041(1)	0.026(3)	0.07	0.04(1)	0.043(5)	0.049(3)	0.130(7)	0.143(4)	0.092(7)
B	3.00	3.00	3.00	3.00	3.00	3.00	3.00	3.00	3.00	3.00	3.00	3.00	3.00	3.00	3.00	3.00	3.00	3.00	3.00
Al	5.36(9)	5.66(9)	6.31(9)	6.32(7)	6.15(5)	6.23(6)	6.50(6)	6.23(6)	7.11(7)	6.1(2)	6.08(5)	5.23(6)	6.63(6)	6.71(9)	6.46(9)	6.43(6)	6.42(5)	6.34(6)	5.73(6)
Cr^{3+}	0.31(3)	0.16(2)	0.001(2)	0.001(2)	0.018(1)	0.015(3)	0.001(1)	0.007(2)	0.001(2)	0.0002(3)	0.0005(5)	0.17(1)	-	-	-	-	0.004(1)	0.007(1)	0.004(2)
V^{3+}	0.79(5)	0.50(3)	0.003(3)	0.002(2)	0.008(3)	0.009(4)	0.004(1)	0.002(2)	0.002(1)	0.007(1)	0.005(2)	0.84(3)	-	-	-	-	0.025(2)	0.036(4)	0.044(2)
Fe^{3+}	-	-	0.077(2)	0.073(2)	0.281(8)	0.25(2)	0.153(5)	0.54(2)	0.143(4)	0.28(2)	0.36(1)	-	0.084(1)	0.087(2)	0.72(2)	0.51(1)	-	-	0.55(1)
Fe^{2+}	0.001(1)	0.002(2)	0.52(1)	0.49(1)	0.57(2)	0.51(4)	0.31(1)	0.01(2)	1.16(3)	1.43(9)	0.44(1)	0.007(4)	1.60(2)	1.65(3)	0.91(2)	1.08(2)	0.33(2)	0.30(4)	0.86(3)
Mn^{2+}	-	0.000(1)	0.004(3)	0.001(1)	0.003(3)	0.007(5)	0.001(2)	0.003(3)	0.051(6)	0.013(3)	0.005(2)	0.002(2)	0.00	0.051(9)	0.021(6)	0.021(9)	0.011(5)	0.010(5)	0.002(2)
Mg	2.56(5)	2.70(6)	2.05(4)	2.07(3)	2.02(2)	2.04(3)	2.11(5)	2.18(3)	0.611(7)	0.9(2)	2.11(2)	2.80(4)	0.67(1)	0.52(6)	0.89(4)	0.90(3)	2.17(2)	2.23(2)	1.78(3)
Zn	-	-	0.01(1)	0.006(8)	0.010(6)	-	0.009(4)	0.005(5)	0.012(8)	0.01(1)	0.008(3)	0.013(8)	0.013(8)	0.038(5)	0.02(1)	0.02(2)	0.02(1)	0.006(6)	0.005(7)
Ca	0.246(6)	0.34(7)	0.077(9)	0.09(2)	0.257(3)	0.263(4)	0.10(2)	0.007(1)	0.010(1)	0.09(6)	0.110(4)	0.412(8)	-	-	-	-	0.151(9)	0.187(3)	0.163(4)
Na	0.46(1)	0.48(1)	0.75(2)	0.72(2)	0.558(9)	0.56(1)	0.71(2)	0.74(1)	0.45(1)	0.68(2)	0.68(1)	0.477(8)	0.633(6)	0.68(3)	0.73(2)	0.71(2)	0.61(2)	0.59(1)	0.73(1)
K	0.012(1)	0.010(4)	0.004(2)	0.003(2)	0.002(2)	0.003(1)	0.004(1)	0.011(1)	0.006(2)	0.009(1)	0.010(2)	0.015(3)	0.013(2)	0.013(2)	0.006(2)	0.009(2)	0.010(1)	0.013(2)	0.005(1)
F	0.08(4)	0.05(4)	0.004(9)	0.05(2)	0.13(3)	0.06(4)	0.004(7)	0.02(1)	0.04(3)	0.21(6)	0.02(2)	0.31(5)	0.18(2)	0.18(4)	0.21(6)	0.157(8)	0.07(2)	0.05(2)	0.04(3)
OH	3.5(2)	3.5(2)	3.6(2)	3.6(2)	3.5(2)	3.5(2)	3.6(2)	3.4(2)	3.5(2)	3.5(2)	3.6(2)	3.2(2)	3.5(2)	3.5(2)	3.0(2)	3.1(2)	3.5(2)	3.4(2)	3.5(2)

Notes: Errors for oxides are standard deviations of repeated analyses on individual crystals. B_2O_3: uncertainty evaluated at 5%. Standard deviation for cations calculated according to Wood and Virgo (1989). Samples TMl2ap, TMl2al, TMl3l, TMl4aa contain Li 0.013(1), 0.025(1), 0.013(1), 0.011(2) apfu, respectively. * Calculated from MS data.

(G), and no less than ± 3 % for doublet areas. Inspection of Mössbauer spectra indicates that all iron is in octahedral coordination (Andreozzi *et al.*, 2002). Based on previous work with borosilicates, results are considered to be reliable within ± 20 % relative (Andreozzi *et al.*, 2000). Contents of FeO and Fe_2O_3 (Table 5) were obtained from Fe^{2+}/Fe^{3+} ratios measured by MS. In a few cases, there was insufficient material to perform Mössbauer analysis and Fe^{2+}/Fe^{3+} ratios were calculated on the basis of stoichiometry.

The unit formulas of Table 5 have been thus calculated on 31 (O, OH, F) assuming: Fe^{2+}/Fe^{3+} ratios from MS data, stoichiometric B_2O_3 (on the basis of examination of structural data, see "Results" for discussion) and, consequently, H_2O contents could be calculated on the basis of charge balance requirements.

For 4 samples (TMl2ap, TMl2al, TMl3l and TMl4aa), Li, B and H have been also measured with an ion microprobe (Bosi, 2001).

Determination of cation distribution

Several procedures may be adopted to determine cation distribution in minerals. Satisfactory results have recently been obtained by combining data from SREF, EMPA and MS (Lavina *et al.*, 2002). This approach simultaneously takes into account both structural and chemical data and reproduces observed parameters by optimising cation distribution. Differences between observed and calculated parameters are minimized using the "chi-square" function (Lavina *et al.*, 2002):

$$F(X_i) = \frac{1}{n}\sum_{j=1}^{n}\left(\frac{O_j - C_j(X_i)}{\sigma_j}\right)^2 \quad (1)$$

where O_j is observed quantity, σ_j its standard deviation, X_i variables, *i.e.*, cation fractions in tetrahedral and octahedral sites, and $C_j(X_i)$ the same quantity as O_j calculated by means of X_i parameters. The n O_j quantities taken into account were: unit cell parameters (a, c), O6 oxygen z coordinate (z_{O6}) and mean bond distances (<T-O>, <Y-O>, <Z-O>) and m.a.n. of T, Y and Z sites, total atomic proportions given by microprobe analyses, and constraints imposed by crystal chemistry (total charge and T, Y and Z site populations). As X site was considered to be populated only by Na, K, Ca and vacancies, it was not included in the minimization procedure.

Mean bond distances were calculated as the linear contribution of each site cation (X_i) multiplied by its specific bond distance (<T-O_i>, <Y-O_i> and <Z-O_i>):

$$\langle T\text{-O}\rangle = \Sigma X_i \langle T\text{-O}\rangle_i \quad (2)$$

$$\langle Y\text{-O}\rangle = \Sigma X_i \langle Y\text{-O}\rangle_i \quad (3)$$

$$\langle Z\text{-O}\rangle = \Sigma X_i \langle Z\text{-O}\rangle_i \quad (4)$$

Table 6. Optimised specific mean bond distances (Å) for schorl-dravite series.

	Si	Ti^{4+}	Al	Cr^{3+} *	V^{3+}	Fe^{3+}	Fe^{2+}	Mg	Mn^{2+}	Zn	Li
<*Y*-O>		[1.966]	1.908	1.978	2.018	2.057	2.139	2.084	[2.191]	[2.101]	[2.121]
<*Z*-O>			1.900	1.970	2.010	2.055	2.131	2.077			
<*T*-O>	1.619		[1.750]								

Notes: Uncertainty of specific mean bond distance was estimated ca. 0.001 Å.
In square brackets: bond distances calculated with Shannon's (1976) radii. Anion dimension is function of constituent-anion radius.
*Both bond distances obtained from examination of Cr- rich samples (Bosi et al., 2004).

In this way a, c and z_{O6} can be expressed as functions of <*T*-O>, <*Y*-O> and <*Z*-O>, the observed values of selected bond distances and atomic coordinates (see Appendix 1). It should be noted that equations of Appendix 1 make up a robust mathematical model, which constrains function (1) to determine the topochemistry compatible with the topology of tourmaline, finding the best "match" between the crystallographic and chemical information.

The following assumptions were made:

1) *T* site was populated by Si and, subordinately, by Al;
2) Li, Zn and Mn^{2+}, given their low quantities and their general preference (Hawthorne, 1996; Hawthorne & Henry, 1999), were fixed in the *Y* site;
3) Cr^{3+} and V^{3+}, when in quantities lower than 0.02 apfu, were fixed in *Y* site.

Because Ti^{4+} was almost always ordered in the *Y* site, particularly in the Ti-richest samples (*e.g.*, TM9840c, TM9840f), it was fixed, in all samples, in *Y* during final minimization runs.

Optimal site assignments have been executed by a quadratic program solver (Optimise tool in Quattro Pro). A first cycle of minimization of equation (1) was performed using bond distances obtained with ionic radii of Shannon (1976). The $F(X_i)$ values ranged from 3 to 46 (with average value of 19), suggesting a reproduction of the structural and chemical parameters qualitatively acceptable, but not within the experimental error. In a second cycle of minimization specific bond distances have been optimised for the major elements. A main routine controlled the D_i variables (<*T*-O_i>, <*Y*-O_i> and <*Z*-O_i>) of Eqs. (2), (3) and (4), to minimize the function:

$$G(X_i,D_i) = \frac{\sum F(X_i)}{(\text{number samples})}$$

These optimised empirical bond distances (Table 6) are valid only for schorl-dravite samples. Final $F(X_i)$ values ranging from 0.10 to 3.10 (with average value of 0.92) were obtained, confirming that almost all (99 %) chemical and structural parameters were reproduced, on average, within their experimental error (a table containing the differences between observed and calculated parameters may be obtained from the authors or through the E.J.M. Editorial Office - Paris); the corresponding site populations are given in Table 7. The final results have been further reconfirmed by different optimisation routine performed using the MINUIT program (James & Roos, 1975).

Table 7. Final assigned site populations for schorl-dravite series.

Sample TM	507c	507e	235a	235b	112a	112c	233g	501e	84a	60e	65e	504c	I2ap	I2al	I3l	I4aa	9840c	9840f	9914b
***X* site**																			
Ca	0.246	0.335	0.077	0.094	0.257	0.263	0.099	0.007	0.010	0.093	0.110	0.412	0.000	0.000	0.000	0.000	0.151	0.187	0.163
Na	0.457	0.479	0.751	0.724	0.558	0.559	0.714	0.742	0.451	0.682	0.677	0.477	0.633	0.678	0.727	0.712	0.605	0.594	0.731
K	0.012	0.010	0.004	0.003	0.002	0.003	0.004	0.011	0.006	0.009	0.010	0.015	0.013	0.013	0.006	0.009	0.010	0.013	0.005
vacancy	0.285	0.176	0.167	0.179	0.183	0.175	0.183	0.240	0.533	0.216	0.204	0.095	0.355	0.309	0.267	0.279	0.234	0.205	0.101
***Y* site**																			
Ti^{4+}	0.024	0.040	0.083	0.062	0.054	0.061	0.038	0.022	0.028	0.081	0.041	0.026	0.052	0.031	0.047	0.051	0.129	0.144	0.090
Al	0.761	0.858	1.231	1.286	0.877	0.931	1.298	1.306	1.546	0.930	1.101	0.621	1.281	1.254	0.947	1.137	1.220	1.252	0.831
Cr^{3+}	0.042	0.064	0.001	0.002	0.018	0.015	0.001	0.007	0.001	0.000	0.001	0.097	0.000	0.000	0.000	0.000	0.004	0.007	0.004
V^{3+}	0.714	0.456	0.003	0.002	0.008	0.009	0.004	0.002	0.002	0.007	0.005	0.574	0.000	0.000	0.000	0.000	0.025	0.015	0.044
Fe^{3+}	0.000	0.000	0.003	0.000	0.283	0.187	0.091	0.379	0.002	0.271	0.291	0.000	0.000	0.000	0.741	0.312	0.000	0.000	0.438
Fe^{2+}	0.001	0.002	0.488	0.485	0.449	0.524	0.329	0.006	1.181	1.223	0.431	0.007	1.500	1.520	0.726	1.095	0.335	0.341	0.859
Mn^{2+}	0.000	0.000	0.004	0.001	0.003	0.008	0.001	0.003	0.054	0.013	0.005	0.002	0.000	0.047	0.024	0.026	0.013	0.011	0.002
Mg	1.458	1.580	1.179	1.152	1.299	1.266	1.228	1.272	0.175	0.459	1.117	1.656	0.142	0.083	0.485	0.346	1.253	1.224	0.721
Zn	0.000	0.000	0.008	0.011	0.009	0.000	0.011	0.003	0.013	0.015	0.008	0.016	0.010	0.038	0.018	0.024	0.021	0.007	0.008
Li	0.000	0.000	0.000	0.000	0.000	0.000	0.000	0.000	0.000	0.000	0.000	0.000	0.013	0.025	0.013	0.011	0.000	0.000	0.000
Σ *Y*	3.000	3.000	3.001	3.000	3.000	3.001	3.001	3.001	3.001	2.998	2.999	2.999	2.999	2.999	3.002	3.002	3.001	3.000	2.998
***Z* site**																			
Al	4.558	4.719	4.984	4.997	5.176	5.145	5.012	4.910	5.385	5.244	4.965	4.540	5.306	5.384	5.380	5.256	5.058	4.989	4.884
Cr^{3+}	0.258	0.096	0.000	0.000	0.000	0.000	0.000	0.000	0.000	0.000	0.000	0.074	0.000	0.000	0.000	0.000	0.000	0.000	0.000
V^{3+}	0.090	0.051	0.000	0.000	0.000	0.000	0.000	0.000	0.000	0.000	0.000	0.260	0.000	0.000	0.000	0.000	0.000	0.021	0.000
Fe^{3+}	0.000	0.000	0.074	0.073	0.000	0.084	0.066	0.155	0.142	0.003	0.061	0.000	0.084	0.087	0.000	0.210	0.000	0.000	0.108
Fe^{2+}	0.000	0.000	0.035	0.017	0.112	0.004	0.000	0.000	0.035	0.232	0.000	0.000	0.085	0.115	0.201	0.000	0.011	0.000	0.000
Mg	1.094	1.135	0.908	0.913	0.712	0.769	0.922	0.936	0.438	0.518	0.973	1.125	0.523	0.412	0.421	0.535	0.931	0.991	1.006
Σ *Z*	6.000	6.001	6.001	6.000	6.001	6.001	6.001	6.001	6.001	5.998	5.999	5.999	5.998	5.999	6.002	6.002	6.001	6.000	5.998
***T* site**																			
Si	5.951	5.952	5.987	5.981	5.857	5.881	5.924	5.999	5.952	5.871	5.955	5.910	5.912	5.836	5.940	5.962	5.937	5.949	5.909
Al	0.049	0.047	0.014	0.020	0.144	0.121	0.075	0.000	0.048	0.128	0.044	0.089	0.087	0.163	0.063	0.040	0.062	0.051	0.089
Σ *T*	6.000	6.000	6.000	6.000	6.001	6.001	6.000	5.999	6.000	5.998	6.000	5.999	5.999	5.999	6.002	6.002	5.999	6.000	5.999
***W* site**																			
O^{2-}	0.383	0.439	0.364	0.382	0.404	0.471	0.362	0.573	0.568	0.352	0.362	0.437	0.311	0.283	0.793	0.703	0.420	0.504	0.449
OH	0.536	0.507	0.632	0.572	0.470	0.469	0.633	0.405	0.395	0.443	0.618	0.248	0.512	0.538	0.000	0.140	0.510	0.442	0.509
F	0.081	0.054	0.004	0.046	0.126	0.060	0.004	0.021	0.038	0.205	0.020	0.314	0.177	0.178	0.207	0.157	0.070	0.054	0.042

Notes: For all samples, $B_3O_{27}{}^{V}OH_3$, except for TMI3l: $^{V}(O_{0.04}OH_{2.96})$. Atomic frequencies are given to the their decimal point for calculation purposes only. For an estimate of the uncertainty refer to standard deviations of table 5.

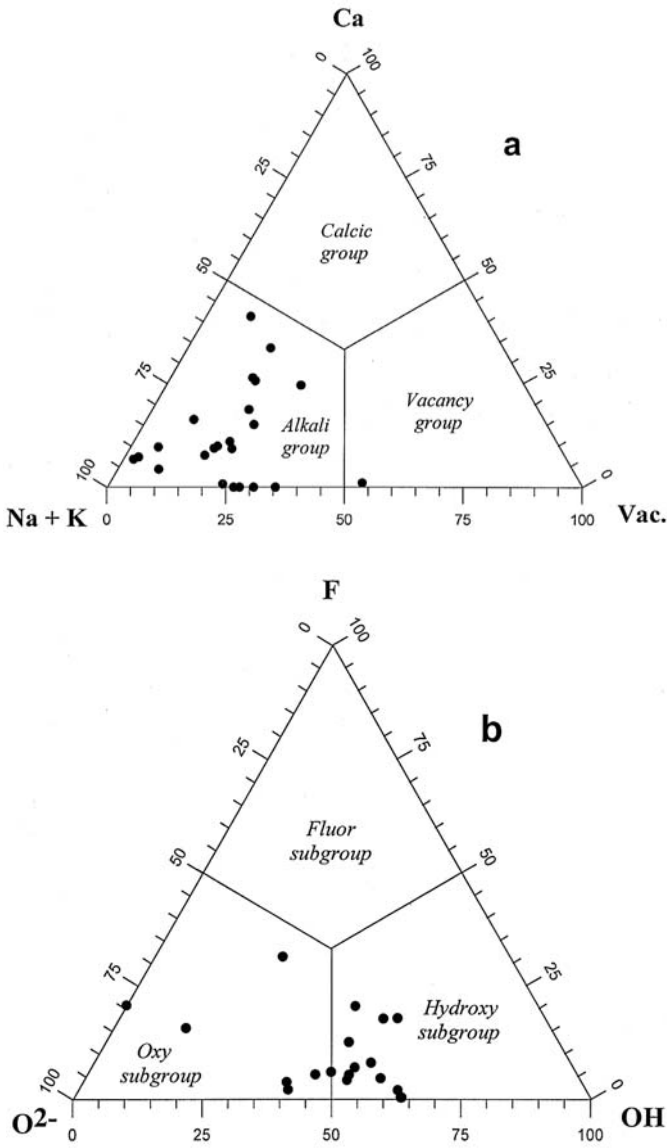

Fig. 1. Diagrams showing the classification of tourmaline according to the principal constituents: a) *X* site; b) *W* site.

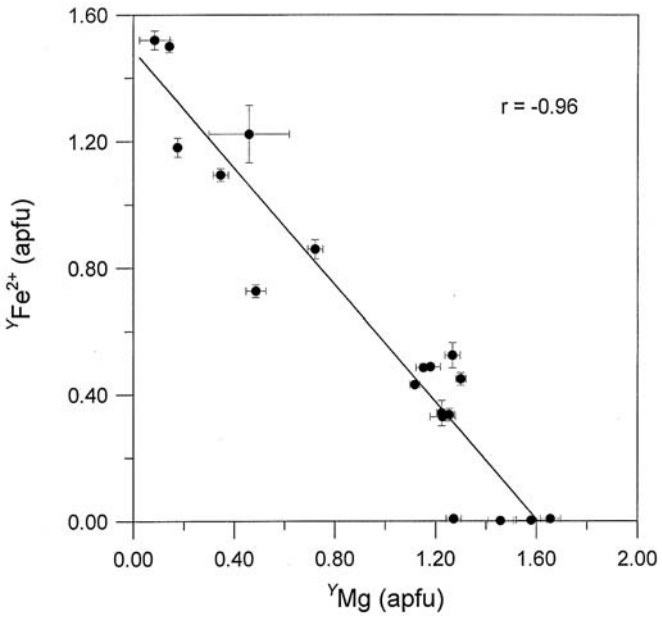

Fig. 2. Relationship between $^{Y}Fe^{2+}$ and ^{Y}Mg shows a replacement next to 1:1, and identifies the tourmalines along the schorl-dravite series.

Results

According to Hawthorne & Henry's (1999) classification, all examined tourmalines belong to the Alkali group, except TM84a, which shows an *X*-site vacancy content of 0.53 (Fig. 1a). Samples belong to the Oxy- and Hydroxy-subgroups (^{W}OH up to 0.6 apfu; F is lower than 0.4 apfu) as may be observed in Fig. 1b. The main substitutions involve the alkali defect ($R^{+} + R^{2+} \leftrightarrow R^{3+} + \square$) and the proton deficient ($OH^{-} + R^{2+} \leftrightarrow R^{3+} + O^{2-}$) types (Foit & Rosenberg, 1977), with correlation coefficients of r = -0.96 and r = -0.99, respectively. Among divalent cations, $^{Y}Mg \leftrightarrow {}^{Y}Fe^{2+}$ (Fig. 2) leads to the two end-members dravite and schorl. In most cases, Fe^{2+} was the dominant form of iron, ranging from 55 to 95 % of total Fe, with one exception, which contained 98 % ferric iron.

As already pointed out, B content was set at stoichiometric values. The hypothesis of B deficiency in *B* site was discarded because the mean bond distance between all examined crystals, <<B-O>> = 1.375(1), is the bond distance typically observed for B in planar triangular coordination in inorganic structures (Hawthorne *et al.*, 1996) and is almost identical (within its standard deviation) to that obtained for tourmaline by Pieczka (1999). Excess B, substituting for Si in *T*, was also discarded on the basis of the observed *T* m.a.n. values and <*T*-O> bond distances, both consistent with Si, Al *T*-site population. This is further verified by the results of the minimization procedure.

Ion microprobe results have highlighted very low contents of Li (< 0.03 apfu), as observed for tourmalines of similar compositions by Dutrow *et al.* (1986). Measured B and H contents resulted identical, within experimental error, to the corresponding calculated ones, confirming the correctness of the previously-described stoichiometric assumptions.

The samples are characterized by a disordered cation distribution (Table 7). *Y* octahedron is mainly populated by Mg (from 0.08 to 1.66 apfu), Fe^{2+} (up to 1.52 apfu), Al (from 0.62 to 1.55 apfu) and, for samples TM507 and TM504, by V^{3+} (from 0.46 to 0.71 apfu). In fact, m.a.n. (from 14.3 to 20.0) and mean bond distance (from 2.004 to 2.046 Å), show that *Y* is occupied, at least partly, by cations smaller than Mg or Fe^{2+}, because the latter have octahedral cation-to-anion bond distances of 2.08 and 2.14 Å, respectively (Shannon, 1976; see also Table 6 for comparison). As already described, the main substitution involves $^{Y}Mg \leftrightarrow {}^{Y}Fe^{2+}$, while no clear substitution was noted between ^{Y}Al and ^{Y}Mg or $^{Y}Fe^{2+}$. The *Z*-octahedron is mainly populated by Mg (from 0.41 to 1.14 apfu) and Al (from 4.54 to 5.39 apfu). In fact, *Z* m.a.n. (from 12.9 to 13.5) and

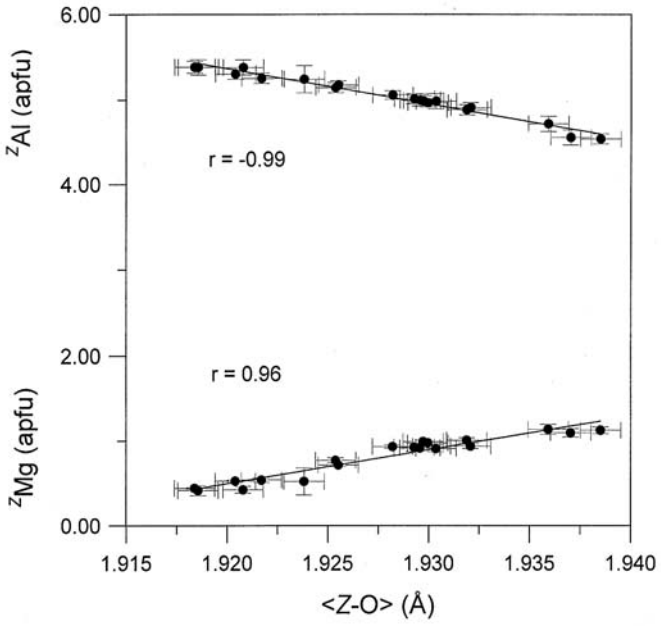

Fig. 3. Relationship between <*Z*-O> and *Z*-site population. An increase in ^{Z}Al results in a contraction of the polyhedron.

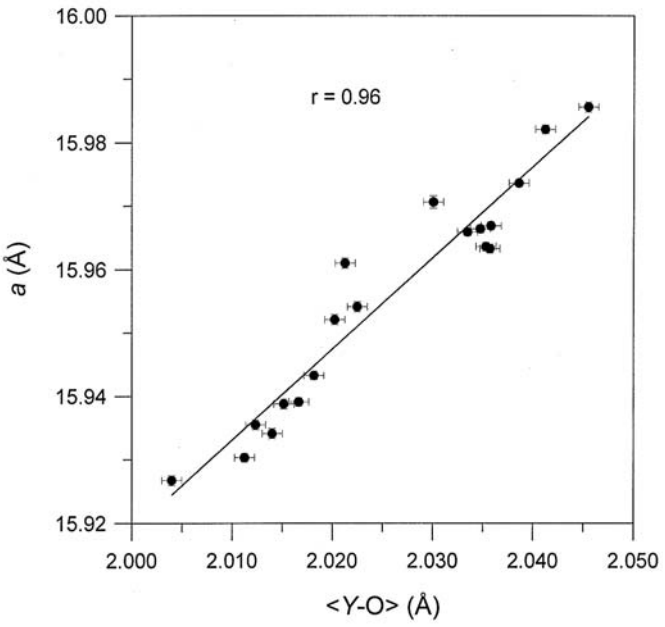

Fig. 4. Variation in *a* cell constant as a function of <*Y*-O> mean bond length.

<*Z*-O> (from 1.918 to 1.939 Å) values are too high to justify full Al occupancy: <*Z*-O> in octahedra entirely occupied by Al, as in elbaite, rossmanite and foitite, ranges from 1.90 to 1.91 Å (Grice & Ercit, 1993; Burns *et al.*, 1994; MacDonald *et al.*, 1993; Selway *et al.*, 1998). Thus, both *Z*-site structural parameters suggest substitution of Al by other larger cations, such as Mg, to account for the longer mean bond distance, and Fe, which may also be responsible for the increase in m.a.n.. Figure 3 shows the relationship between <*Z*-O> and its site population: *Z*-size increases with ^{Z}Mg and decreases with ^{Z}Al.

Cation intracrystalline distribution has many effects not only on the geometry of *Y* and *Z* but on the entire structure of tourmaline. Octahedral dimensions act on unit cell parameters; *a* depends on *Y* size: $a = 13.045 + 1.437$ <*Y*-O> (Fig. 4), whereas *c* is correlated with *Z* size: $c = 0.886 + 3.272$ <*Z*-O> (Fig. 5). The same holds for *Y* and *Z* volumes ($a = 14.932 + 0.096\ V_Y$, r = 0.97 and $c = 5.026 + 0.232\ V_Z$, r = 0.96).

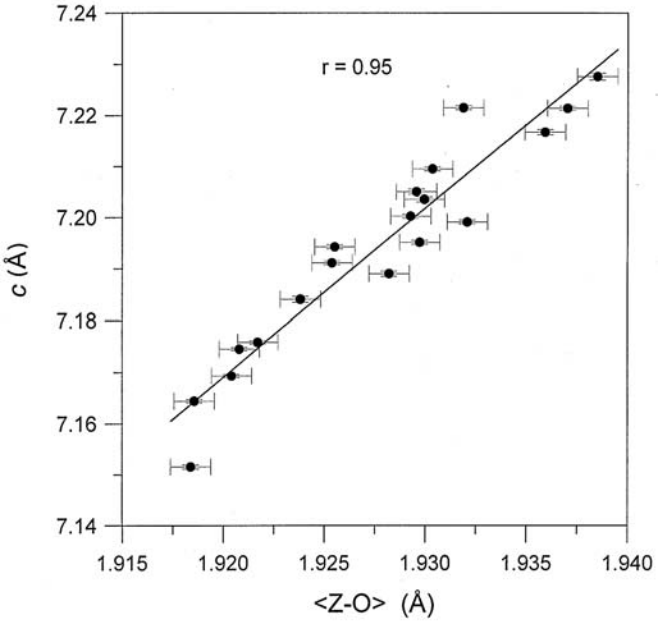

Fig. 5. Variation in *c* cell constant as a function of <*Z*-O> mean bond length.

Discussion and conclusions

In schorl-dravite series, major elements (Al, Fe, Mg) are distributed, with different degrees of preference, among the *Z* and *Y* octahedra: Al populates both sites, with a marked preference for the smaller *Z* octahedron; Mg shows nearly equal distribution between *Y* and *Z* sites. Fe^{2+} and Fe^{3+} populate both *Y* and *Z* sites, but show a strong preference for *Y*. In samples where Al content exceeds 6 apfu, the *Z* site should not be assumed to be fully occupied by Al.

Y size is dependent on the cooperative effect of the various cations populating the site. This effect results in a size contraction due to ^{Y}Al content, along different trends characterized by: $^{Y}Fe^{2+}$, ^{Y}Mg and $^{Y}V^{3+}$ (Fig. 6). The size decrease of this octahedron with progressive increase in ^{Y}Al, is evidenced by the contraction of its edges (*e.g.*, <*Y*-O> *vs.* O1-O2B, r = 0.99) and O3-O6 (r = 0.84). As a quantitative measure of the octahedral and tetrahedral distortion, quadratic elongation <λ>, was adopted because it is the "true measure of polyhedral distortion" (Robinson *et al.*, 1971). Octahedral distortion $<\lambda_Y>$ is inversely corre-

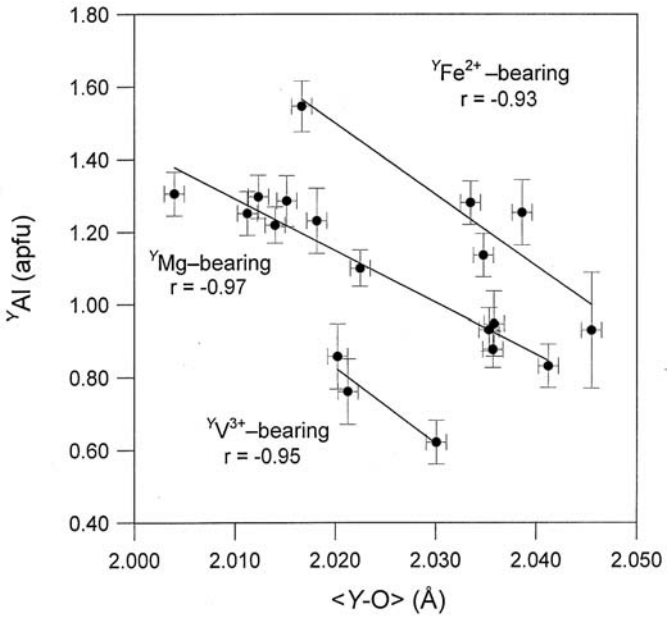

Fig. 6. *Y* size decreases with ^{Y}Al content, evidencing different trends linked to the other cations populating the site: $^{Y}Fe^{2+}$–bearing (1.52 – 1.09 apfu), ^{Y}Mg–bearing (1.30 – 0.49 apfu) and $^{Y}V^{3+}$–bearing (0.71 – 0. 47 apfu).

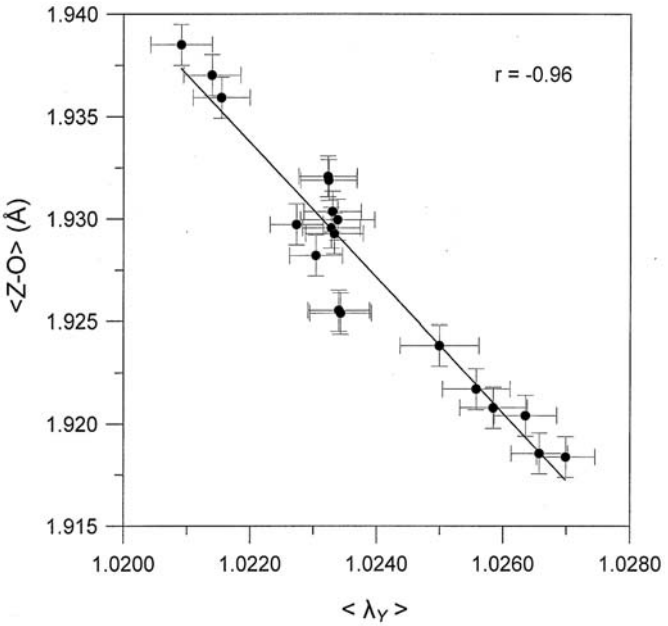

Fig. 8. Relationship between $<\lambda_Y>$ and <*Z*-O>, showing the influence of the second coordination sphere on the *Y*-polyhedron distortion.

lated with ^{Y}Mg, the less covalent cation (r = –0.95) - that is, to the dravite component. Despite its dependency on ^{Y}Mg content, quadratic elongation does not depend on polyhedral dimensions. Unlike the situation for *Y*, *Z* dimensional variation is well described by its bond distances, except for *Z*-O7D, which is independent of *Z* size and sensitive only to ^{Y}Al content (r = –0.86), and thus does not reflect *Z* topochemistry. *Z* size is correlated to *Z* edges, except O3-O6 and O3-O8. The former edge, O3-O6, is the only parameter inversely correlated with *Z* distortion $<\lambda_Z>$ (r = –0.94). The two octahedra mutually interact by means of their common edge O3-O6, any decrease in which, being dependent on *Y* size and thus on ^{Y}Al content, results in larger *Z* distortions. Instead, *Y* distortion is correlated with ^{Z}Al content (r = 0.93) - that is, *Z* size.

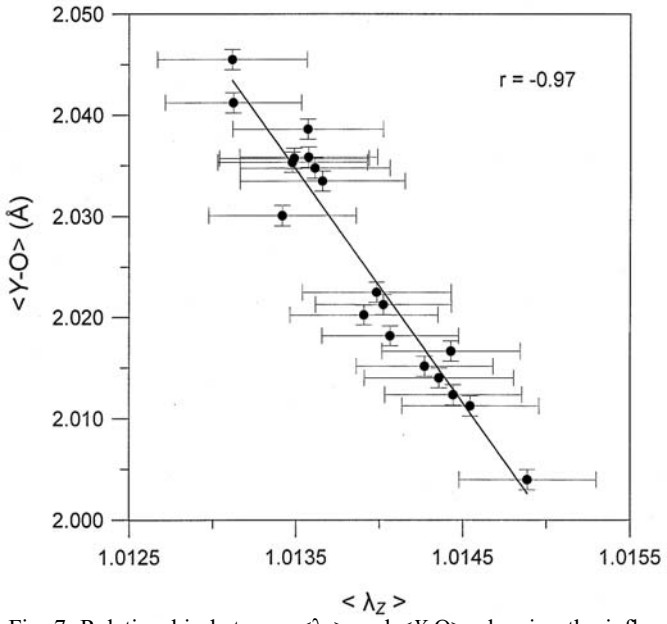

Fig. 7. Relationship between $<\lambda_Z>$ and <*Y*-O>, showing the influence of the second coordination sphere on the *Z*-polyhedron distortion.

In the schorl-dravite series, structural variations mostly appear to be due to *Y* and *Z* interactions. These effects are conspicuous over the entire structure, as *Y* dimensions directly affect the *a* cell parameter, while *Z* is similarly correlated with *c*. The dimensions of both octahedra are correlated with their respective chemical contents. This is particularly evident for *Z*, for which linear relationships were observed between Al or Mg contents and <*Z*-O>. In the case of *Y*, these interactions were less obvious because site populations are extremely variable. Instead, both octahedra interact reciprocally influencing their distortions: conspicuous correlations exist between <*Y*-O> and $<\lambda_Z>$ (Fig. 7) and <*Z*-O> and $<\lambda_Y>$ (Fig. 8). As a general rule, the effects of the octahedral second coordination sphere are confined to polyhedral distortions instead of dimensional variations, which only depend on site populations.

Acknowledgements: Dr. A. Koneva, Institute of Geochemistry, Russian Academy of Sciences, Irkutsk, Russia; Prof. G. Graziani, University of Rome, Italy; Prof. Jùlio César-Mendes, DEGEO, Escola de Minas, UFOP, Campus do Morro do Cruzeiro, Ouro Preto, Minas Gerais, Brazil, are thanked for kindly furnishing samples. The authors also wish to express their gratitude to the Director of the "Museo di Mineralogia" of the University of Rome "La Sapienza", for making available the other samples.

Prof. U. Russo, University of Padova and Dr. G.B. Andreozzi, University of Rome "La Sapienza", Italy, collected Mössbauer spectra. The authors are grateful to Prof. A. Della Giusta, University of Padova and two referees, Prof. B. Dutrow and Prof. I. Puschharovskii, whose suggestions greatly improved the manuscript. This work was supported by a MURST grant.

References

Andreozzi, G.B., Ottolini, L., Lucchesi, S., Graziani, G., Russo, U. (2000): Crystal chemistry of the axinite-group minerals: A multi-analytical approach. *Am. Mineral.*, **85**, 698-706.

Andreozzi, G.B., Bosi, F., Graziani, G., Lucchesi, S. (2002): Order-disorder of Al, Mg, Fe^{2+} and Fe^{3+} and site interactions in the borosilicates axinite and tourmaline. *Proceedings 18th General Meeting of the International Mineralogical Association (Edimburgh)*.

Barton, R., Jr. (1969): Refinement of the crystal structure of buergerite and the absolute orientation of tourmalines. *Acta Cryst.*, **B25**, 1524-1533.

Bloodaxe, E.S., Hughes, J.M., Dyar, M.D., Grew, E.S., Guidotti, C.V. (1999): Linking structure and chemistry in the Schorl-Dravite series. *Am. Mineral.*, **84**, 922-928.

Bosi, F. (2001): Crystal chemistry of the minerals of the tourmaline group. 176 p. Ph. D. dissertation, University from Rome "La Sapienza", Rome (in Italian).

Bosi, F., Lucchesi, S., Reznitskii, L. (2004): Crystal chemistry of the dravite – chromdravite series. *Eur. J. Mineral.*, **16**, 345-352.

Burns, P.C., MacDonald, D.J., Hawthorne, F.C. (1994): The crystal chemistry of manganese-bearing elbaite. *Can. Mineral.*, **32**, 31-41.

Dutrow, B.L., Holdaway, M.J., Hinton, R.W. (1986): Lithium in staurolite and its petrologic significance. *Contrib. Mineral. Petrol.*, **94**, 496-506.

Foit, F.F., Jr. (1989): Crystal chemistry of alkali-deficient schorl and tourmaline structural relationships. *Am. Mineral.*, **74**, 422-431.

Foit, F.F., Jr. & Rosenberg, P.E. (1977): Coupled substitutions in the tourmaline group. *Contrib. Mineral. Petrol.*, **62**, 109-127.

Grice, J.D. & Ercit, T.S. (1993): Ordering of Fe and Mg in the tourmaline crystal structure: The correct formula. *N. Jb. Mineral. Abh.*, **165**, 245-266.

Hawthorne, F.C. (1996): Structural mechanisms for light-element variations in tourmaline. *Can. Mineral.*, **34**, 123-132.

Hawthorne, F.C. & Henry D. (1999): Classification of the minerals of the tourmaline group. *Eur. J. Mineral.*, **11**, 201-215.

Hawthorne, F.C., MacDonald, D.J., Burns, P.C. (1993): Reassignment of cation site occupancies in tourmaline: Al-Mg disorder in the crystal structure of dravite. *Am. Mineral.*, **78**, 265-270.

Hawthorne, F.C., Burns, P.C., Grice, J.D. (1996): The crystal chemistry of boron. *In* "Boron: Mineralogy, Petrology and Geochemistry, Reviews in Mineralogy, 33", L.M. Anovitz & E.S. Grew, eds. Mineralogical Society of America, 41-115.

James, F. & Roos, M. (1975): Minuit-A system for function minimization and analysis of the parameter errors and correlations. *Comp. Phys. Comm.*, **10**, 343-367.

Lavina, B., Salviulo, G., Della Giusta, A. (2002): Cation distribution and structure modelling of spinel solid solutions. *Phys. Chem. Minerals*, **29**, 10-18.

MacDonald, D.J. & Hawthorne, F.C. (1995): The crystal chemistry of Si ↔ Al substitution in tourmaline. *Can. Mineral.*, **33**, 849-858.

MacDonald, D.J., Hawthorne, F.C., Grice, J.D. (1993): Foitite, $\square[Fe^{2+}_2(Al,Fe^{3+})]$ $Al_6Si_6O_{18}(BO_3)_3(OH)_4$, a new alkali-deficient tourmaline: Description and crystal structure. *Am. Mineral.*, **78**, 1299-1303.

Pieczka, A. (1999): Statistical interpretation of structural parameters of tourmalines: the ordering of ions in the octahedral sites. *Eur. J. Mineral.*, **11**, 243-251.

— (2000): Modelling of some structural parameters of tourmalines on the basis of their chemical composition. I. Ordered structure model. *Eur. J. Mineral.*, **12**, 589-596.

Pouchou, J.L. & Pichoir, F. (1984): A new model for quantitative X-ray micro-analysis. I. Application to the analysis of homogeneous samples. *La Recherche Aérospatiale*, **3**, 13-36.

Robinson, K., Gibbs, G.V., Ribbe, P.H. (1971): Quadratic elongation: a quantitative measure of distortion in coordination polyhedra. *Science*, **172**, 567-570.

Selway, J.B., Novàk, M., Hawthorne, F.C., Černý, P., Ottolini, L., Kyser, T.K. (1998): Rossmanite, $\square(LiAl_2)Al_6(Si_6O_{18})(BO_3)_3(OH)_4$, a new alkali-deficient tourmaline: Description and crystal structure. *Am. Mineral.*, **83**, 896-900.

Shannon, R.D. (1976): Revised effective ionic radii and systematic studies of interatomic distances in halides and chalcogenides. *Acta Cryst.*, **A32**, 751-767.

Taylor, M.C., Cooper, M.A., Hawthorne, F.C. (1995): Local charge-compensation in hydroxyl-deficient uvite. *Can. Mineral.*, **33**, 1215-1221.

Wood, B.J. & Virgo, D. (1989): Upper mantle oxidation state: Ferric iron contents of lherzolite spinels by ^{57}Fe Mössbauer spectroscopy and resultant oxygen fugacity. *Geochim. Cosmochim. Acta*, **53**, 1277-1291.

Received 16 April 2003
Modified version received 29 October 2003
Accepted 27 November 2003

Appendix 1: Geometrical relations in tourmaline structure.

From the definition of mean bond distance for *Z*, *Y* and *T* polyhedrons of tourmaline:

$\langle Z\text{-O}\rangle = (ZO3 + ZO6 + ZO7D + ZO7E + ZO8 + ZO8E)/6$ (1)

$\langle Y\text{-O}\rangle = (YO1 + 2\cdot YO2 + YO3 + 2\cdot YO6)/6$ (2)

$\langle T\text{-O}\rangle = (TO4 + TO5 + TO6 + TO7)/4$ (3)

The bond distances *ZO*6, *YO*6 and *TO*6, can be expressed as a function of fractional coordinates (x, y, z) and unit cell parameters (a, c):

$(ZO6)^2 = [(x_Z - x_{O6})^2 + (y_Z - y_{O6})^2 - (x_Z - x_{O6})(y_Z - y_{O6})]\, a^2 + (z_Z - z_{O6})^2 c^2$

$(YO6)^2 = [(x_Y - x_{O6})^2 + (1/2\, x_Y - y_{O6})^2 - (x_Y - x_{O6})(1/2\, x_Y - y_{O6})]\, a^2 + (z_Y - z_{O6})^2 c^2$

$(TO6)^2 = [(x_T - x_{O6})^2 + (y_T - y_{O6})^2 - (x_T - x_{O6})(y_T - y_{O6})]\, a^2 + (1 - z_{O6})^2 c^2$

Considering constants z_Z, z_Y and the quantities:

$ZZZ = [(x_Z - x_{O6})^2 + (y_Z - y_{O6})^2 - (x_Z - x_{O6})(y_Z - y_{O6})]$

$YYY = [(x_Y - x_{O6})^2 + (1/2\, x_Y - y_{O6})^2 - (x_Y - x_{O6})(1/2\, x_Y - y_{O6})]$

$TTT = [(x_T - x_{O6})^2 + (y_T - y_{O6})^2 - (x_T - x_{O6})(y_T - y_{O6})]$

$SZ = ZO3 + ZO7D + ZO7E + ZO8 + ZO8E$

$SY = 1/2\,(YO1) + YO2 + 1/2\,(YO3)$

$ST = TO4 + TO5 + TO7$

we can replace these terms and express equations (1), (2) and (3) in the following way:

$(ZZZ)\ a^2 + (z_Z - z_{O6})^2 c^2 = [6\langle Z\text{-O}\rangle - (SZ)]^2$ (4)

$(YYY)\ a^2 + (z_Y - z_{O6})^2 c^2 = [3\langle Y\text{-O}\rangle - (SY)]^2$ (5)

$(TTT)\ a^2 + (1 - z_{O6})^2 c^2 = [4\langle T\text{-O}\rangle - (ST)]^2$ (6)

Equation (4), (5) and (6) make up a system in three unknowns (a, c, z_{O6}), whose solution is:

$$zo6 := \frac{1}{2}\left(-32\,YYY\,TO^2\,zz - 2\,SY^2\,ZZZ - 16\,zy\,ZZZ\,TO\,ST - 24\,YYY\,ZO\,SZ + 72\,YYY\,ZO^2 + 2\,YYY\,SZ^2 - 2\,zy\,TTT\,SZ^2 + 2\,zy\,ZZZ\,ST^2 - 72\,zy\,TTT\,ZO^2 + 24\,zy\,TTT\,ZO\,SZ + 16\,YYY\,TO\,ST\,zz + 12\,YO\,SY\,ZZZ - 18\,YO^2\,ZZZ + 18\,YO^2\,TTT\,zz + 32\,zy\,ZZZ\,TO^2 - 2\,YYY\,ST^2\,zz + 2\,SY^2\,TTT\,zz - 12\,YO\,SY\,TTT\,zz - \left((32\,YYY\,TO^2\,zz + 2\,SY^2\,ZZZ + 16\,zy\,ZZZ\,TO\,ST + 24\,YYY\,ZO\,SZ - 72\,YYY\,ZO^2 - 2\,YYY\,SZ^2 + 2\,zy\,TTT\,SZ^2 - 2\,zy\,ZZZ\,ST^2 + 72\,zy\,TTT\,ZO^2 - 24\,zy\,TTT\,ZO\,SZ - 16\,YYY\,TO\,ST\,zz - 12\,YO\,SY\,ZZZ + 18\,YO^2\,ZZZ - 18\,YO^2\,TTT\,zz - 32\,zy\,ZZZ\,TO^2 + 2\,YYY\,ST^2\,zz - 2\,SY^2\,TTT\,zz + 12\,YO\,SY\,TTT\,zz\right)^2 - 4\left(-36\,ZO^2\,TTT - SZ^2\,TTT + 9\,YO^2\,TTT + SY^2\,TTT + 36\,YYY\,ZO^2 - 12\,YYY\,ZO\,SZ + YYY\,SZ^2 + 16\,ZZZ\,TO^2 - 8\,ZZZ\,TO\,ST + ZZZ\,ST^2 + 12\,ZO\,SZ\,TTT - 16\,YYY\,TO^2 + 8\,YYY\,TO\,ST - YYY\,ST^2 - 9\,YO^2\,ZZZ + 6\,YO\,SY\,ZZZ - 6\,YO\,SY\,TTT - SY^2\,ZZZ\right)\left(-36\,zy^2\,TTT\,ZO^2 - zy^2\,TTT\,SZ^2 + 36\,YYY\,ZO^2 + YYY\,SZ^2 + 9\,YO^2\,TTT\,zz^2 - 9\,YO^2\,ZZZ + SY^2\,TTT\,zz^2 - SY^2\,ZZZ + 16\,zy^2\,ZZZ\,TO^2 - 8\,zy^2\,ZZZ\,TO\,ST + zy^2\,ZZZ\,ST^2 + 12\,zy^2\,TTT\,ZO\,SZ - 12\,YYY\,ZO\,SZ - 16\,YYY\,TO^2\,zz^2 + 8\,YYY\,TO\,ST\,zz^2 - YYY\,ST^2\,zz^2 - 6\,YO\,SY\,TTT\,zz^2 + 6\,YO\,SY\,ZZZ\right)\right)^{1/2}\Big)\Big/\left(-36\,ZO^2\,TTT - SZ^2\,TTT + 9\,YO^2\,TTT + SY^2\,TTT + 36\,YYY\,ZO^2 - 12\,YYY\,ZO\,SZ + YYY\,SZ^2 + 16\,ZZZ\,TO^2 - 8\,ZZZ\,TO\,ST + ZZZ\,ST^2 + 12\,ZO\,SZ\,TTT - 16\,YYY\,TO^2 + 8\,YYY\,TO\,ST - YYY\,ST^2 - 9\,YO^2\,ZZZ + 6\,YO\,SY\,ZZZ - 6\,YO\,SY\,TTT - SY^2\,ZZZ\right)$$

$$a := \left(\left(36\,ZO^2 + 72\,zo6\,ZO^2\,zy - SY^2 + SZ^2 - 9\,YO^2 - 72\,zo6\,ZO^2 + 18\,zo6\,YO^2 + 16\,zy^2\,TO^2 + 9\,zz^2\,YO^2 - 36\,ZO^2\,zy^2 - 16\,zz^2\,TO^2 - SZ^2\,zy^2 + zy^2\,ST^2 - zz^2\,ST^2 + zz^2\,SY^2 + 2\,zo6\,SY^2 - 2\,zo6\,SZ^2 + 6\,YO\,SY - 12\,ZO\,SZ - 18\,zo6\,zz\,YO^2 + 32\,zo6\,zz\,TO^2 - 32\,TO^2\,zy\,zo6 - 2\,zo6\,zz\,SY^2 + 2\,zo6\,zz\,ST^2 - 12\,zo6\,YO\,SY - 2\,ST^2\,zy\,zo6 + 12\,SZ\,ZO\,zy^2 + 2\,zo6\,SZ^2\,zy - 8\,zy^2\,TO\,ST - 6\,zz^2\,YO\,SY + 8\,zz^2\,TO\,ST + 24\,zo6\,ZO\,SZ - 16\,zo6\,zz\,TO\,ST + 12\,zo6\,zz\,YO\,SY + 16\,TO\,ST\,zy\,zo6 - 24\,zo6\,ZO\,SZ\,zy\right)\Big/\left(2\,TTT\,zz\,zo6 + zy^2\,TTT - zz^2\,TTT - 2\,zy\,zo6\,TTT - ZZZ\,zy^2 + ZZZ + 2\,YYY\,zo6 + YYY\,zz^2 + 2\,ZZZ\,zy\,zo6 - YYY - 2\,zo6\,ZZZ - 2\,YYY\,zz\,zo6\right)\right)^{1/2}$$

$$c := \left(\left(-36\,ZO^2\,TTT - SZ^2\,TTT + 9\,YO^2\,TTT + SY^2\,TTT + 36\,YYY\,ZO^2 - 12\,YYY\,ZO\,SZ + YYY\,SZ^2 + 16\,ZZZ\,TO^2 - 8\,ZZZ\,TO\,ST + ZZZ\,ST^2 + 12\,ZO\,SZ\,TTT - 16\,YYY\,TO^2 + 8\,YYY\,TO\,ST - YYY\,ST^2 - 9\,YO^2\,ZZZ + 6\,YO\,SY\,ZZZ - 6\,YO\,SY\,TTT - SY^2\,ZZZ\right)\Big/\left(2\,TTT\,zz\,zo6 + zy^2\,TTT - zz^2\,TTT - 2\,zy\,zo6\,TTT - ZZZ\,zy^2 + ZZZ + 2\,YYY\,zo6 + YYY\,zz^2 + 2\,ZZZ\,zy\,zo6 - YYY - 2\,zo6\,ZZZ - 2\,YYY\,zz\,zo6\right)\right)^{1/2}$$

where: $zo6 = z_{O6}$, $zy = z_Y$, $zz = z_Z$, $TO = \langle T\text{-O}\rangle$, $YO = \langle Y\text{-O}\rangle$, $ZO = \langle Z\text{-O}\rangle$.

Only the relation concerning z_{O6} is totally explicit, whereas the others, for the sake of brevity, are reported in terms of z_{O6} parameter, and must be developed in sequence.